Journal of Fluorescence (2022) 32:1155–1169
https://doi.org/10.1007/s10895-022-02916-3

ORIGINAL ARTICLE

Study on Photophysical Properties of Novel Fluorescent Phenanthroimidazole-Thiadiazole Hybrid Derivatives

Merve Zurnacı[1] · İzzet Şener[2] · Mahmut Gür[3] · Nesrin Şener[4]

Received: 21 December 2021 / Accepted: 25 February 2022 / Published online: 24 March 2022

Abstract

Phenanthroimidazole-thiadiazole hybrid derivatives, which are new heterocyclic compounds with fluorescence properties, were synthesized by designing a two-step reaction mechanism and their photophysical properties were investigated. The synthesized derivatives were purified and their structures were elucidated by ATR-IR, ^{1}H-NMR, elemental analysis and HR-MS methods. In the next stage of the study, the absorption and emission spectra of the synthesized new phenanthroimidazole-thiadiazole hybrid derivatives were determined by UV–Vis and fluorescence spectroscopy. Stokes' shifts, molar extinction coefficients (ε), singlet energy levels (Es), quantum yield (ϕ_f), lifetimes (τ), the radiative (k_r) and the nonradiative (k_{nr}) constant for new hybrid derivatives were measured in DMSO. In addition, aggregation measurements, which is an important parameter that changes the photophysical properties were performed and for these compounds, structure: photophysical properties were discussed.

Keywords Phenanthroimidazole-thiadiazole · Blue fluorescence · Quantum yield · Fluorescence lifetimes · Photophysical properties · Aggregation

Introduction

Fluorescent organic materials are of great interest in modern science and developing technology due to their photophysical and electrochemical properties [1–4]. Major application areas such as biological imaging probes, sensors, lasers, organic light emitting devices (OLEDs), organic field-effect transistors (OFETs), organic photovoltaic devices and nanoemitters have been developed as a result of this interest [5–9]. The design and synthesis of new fluorescent organic materials is an important step in the development of new generation technological applications [10]. Therefore, organic materials are required as new and different building blocks [11]. Among these organic materials, heterocyclic compounds play an important role with their effective quantum yields, high π conjugation system and strong absorption and emission properties in the visible region [12]. In addition, the ability to simultaneously adjust the fluorescence color and intensity of heterocyclic compounds makes them suitable for use in OLEDs and bio-imaging or as chemosensors and fluorophores in the detection of various elements [13]. In heterocyclic compounds, especially nitrogen-containing heterocyclic compounds stand out due to their optical properties [14]. Among them, it has been discovered that phenanthroimidazole and its derivatives, which are molecules containing planar aromatic rings, exhibit strong photophysical properties that can be altered by intramolecular or intermolecular interaction [15].

Phenanthroimidazole consists of a thermally stable phenanthrene structure and an imidazole ring [15]. The imidazole group is highly polar and electron withdrawing due to the presence of an electronegative nitrogen atom [16]. Phenanthroimidazole is widely used to obtain fluorescent materials with high efficiency due to its structure, good electron withdrawing ability, large Stokes' shift, high quantum

✉ Merve Zurnacı
mzurnaci@kastamonu.edu.tr

[1] Central Research Laboratory, Kastamonu University, 37200 Kastamonu, Turkey

[2] Department of Food Engineering, Faculty of Engineering and Architecture, Kastamonu University, 37200 Kastamonu, Turkey

[3] Department of Forest Industrial Engineering, Faculty of Forestry, Kastamonu University, 37200 Kastamonu, Turkey

[4] Department of Chemistry, Faculty of Art and Science, Kastamonu University, 37200 Kastamonu, Turkey

yield, excellent thermal properties and good color purity in the dark blue area [17–20]. Phenanthroimidazole and its derivatives are also used as host materials in OLEDs and as donors for dye-sensitized solar cells [21]. With these properties, phenanthroimidazole compounds have emerged as promising fluorescent molecules and their photophysical properties have become the focus of attention of researchers [22–24]. Thiadiazole compounds have advantages such as high chemical and thermal stability allowing structural modifications and electron accepting tendencies among heterocyclic compounds [25]. Because of these properties, it is of great importance in the design of new fluorescent organic materials [26, 27].

Our previous study has already reported synthesis and fabricated thin film (glass/ITO) and of surface and optoelectronic properties of compound, prepared from 9,10-phenanthrenequinone, 4-carboxybenzaldehyde and 2-phenylethyl thiosemicarbazide [28]. In this study, new series phenanthroimidazole-thiadiazole hybrids were designed and synthesized. Synthesized compounds were characterized by spectroscopic techniques (ATR-IR, ^{1}H-NMR, HR-MS). The absorption and steady-state emission spectra of the compounds were recorded in different polarity solvent. We report herein their photophysical properties such as fluorescence quantum yields and lifetimes were also determined in DMSO. In order to examine the aggregation properties of the compounds, measurements were made in solution at different concentrations (in UV region). Also, the relationship between the molecular structures and their photophysical properties of the designed fluorescent compounds was investigated.

Experimental

Chemicals and Equipments

All the materials for synthesis, purification step, absorption and emission measurements, quantum yield, lifetime measurement were of analytical grade and purchased from commercial suppliers (from Sigma-Aldrich and Merck). The compounds were investigated by thin layer chromatography (TLC) using Kieselgel-60 GF254 (Merck). The melting point of the compounds was measured by Stuart SMP30 instrument. Percentages of the elements C, H, and N (elemental analysis) were performed using Eurovector Brand EA3000-Single Model. NMR analyses were performed using Bruker Ultrashield 300 MHz NMR spectrometer. Fourier-transform infrared (ATR-IR) analyses were recorded on using the Bruker Alpha instrument at room temperature. Mass results were obtained by carrying analysis on Shimadzu, LCMS-8030 Plus Series.

Photophysical Measurements

The absorption spectra of the compounds were determined with Shimadzu UV Pharmaspec 1700. Steady-state fluorescence was measured by a Horiba Fluoromaks-4 fluorescence spectrophotometer. Excitation and emission slit widths and integration time were set at 1 nm band pass and 0,1 s respectively. The concentration of **PHN1a-o** derivatives was 1.0×10^{-5} M in DMSO solution and measurements were taken at room temperature.

Time-resolved fluorescence lifetimes measurements were performed on FS5, Edinburgh Instruments with laser excitation at 400 nm. Nanosecond fluorescence lifetimes were measured with decay scan and the following settings values: total experiment time, 124,20 s; excitation and emission band widths, 8 nm. The solvent used in the photophysical measurements were spectroscopic grade.

In this study, the quantum yield for synthesis compound in DMSO was determined using the following equation (Eq. (1)) for reference and sample solutions at concentrations of 1.0×10^{-5} M [29]. Perylene in cyclohexane ($\Phi_f=0.94$) was used as a reference [30, 31].

$$\Phi_{\ddot{o}} = \frac{A_s I_{\ddot{o}} \left(n_{\ddot{o}}\right)^2}{A_{\ddot{o}} I_s \left(n_s\right)^2} \Phi_s \tag{1}$$

In addition, the aggregation behavior of the synthesized phenanthroimidazole-thiadiazole hybrid derivatives (**PHN1a-o**) were determined in DMSO. The variation of UV–Vis spectral measurements in the range of 2.0×10^{-5} M-1.0×10^{-6} M at 7 different concentrations was investigated.

Synthesis of Phenanthroimidazole-thiadiazole Hybrid Derivatives

Synthesis of 4-(1H-phenanthro[9,10-d]imidazol-2-yl) Benzoic Acid (Compound PHN)

9,10-phenanthrenequinone (1 g, 4.80 mmol), 4-bromobenzaldehyde (0,72 g, 4.80 mmol), ammonium acetate (7,4 g, 96 mmol) and glacial acetic acid (60 mL) were added into 100 mL round-bottomed flask. The reaction mixture was stirred under reflux for 4 h at 90–100 °C [19, 32]. The product was released to cool to room temperature (25 ºC) and then poured into ice-water mix. Obtained solid product was collected by filtration, washed with water and then dried. The drying process was carried out in a vacuum oven for 24 h. $C_{22}H_{14}N_2O_2$ (338.36 g/mol); light yellow solid; yield 53.7%; m.p.: > 360 ºC [19].

Synthesis of Thiosemicarbazide Compounds (Compounds 1a-o)

Thiosemicarbazide compounds were synthesized according to the method specified in the literature [33]. Equivalent moles of isothiocyanate were dissolved in 10 mL ethanol in a 100 mL beaker and placed in an ice bath. In another beaker, hydrazine monohydrate was dissolved in 10 mL ethanol and added dropwise to the isothiocyanate mixture. The reaction was terminated after 2 h and kept in the refrigerator for 24 h. It was then filtered and dried in a vacuum oven.

Synthesis of Phenanthroimidazole Thiadiazole Hybrid Compounds (Compounds PHN1a-o)

Compound PHN (n mol), thiosemicarbazide (n mol) were allowed to stir under reflux for 4 h at 90 °C in the presence of $POCl_3$ (3n mol). It was stirred under reflux for 4 h. The mixture was cooled to room temperature and precipitated with ice. It was neutralized by the dropwise addition of 20% ammonia solution. The precipitates were filtered, washed with water and passed through diethyl ether. It was left in a vacuum oven for 24 h to dry. The resulting product was monitored by using thin-layer chromatography and purified by crystallization pure

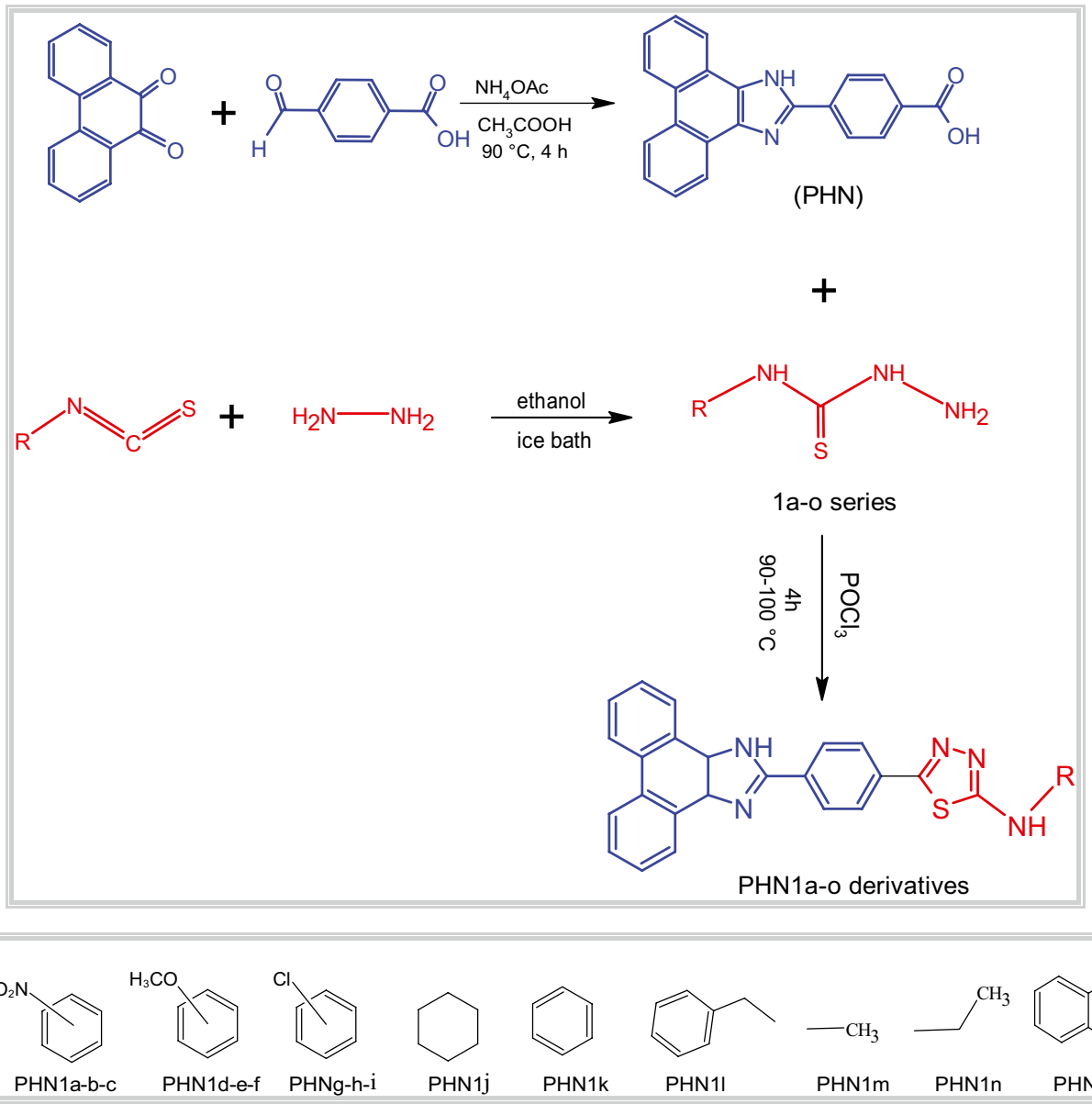

Scheme 1 Structure and synthesis route of PHN1a-o derivatives

compounds **PHN1a-o**. The products were obtained different color crystals in 77–91% yields. Structure and synthesis route of **PHN1a-o** derivatives are given in the Scheme 1.

5-(4-(1H-phenanthro[9,10-d]imidazol-2-yl)phenyl)-2-nitrophenyl-1,3,4-thiadiazol-2-amine) (PHN1a)

Red powder and purified in DMSO-water. Yield: (79%), melting point (mp): 273 ºC; **ATR-IR (ν_{maks}, cm^{-1}):** 3351.56, 3248.71 (stretching, -NH); 3056.90 (Aromatic C-H); 1650.35 (bending, -NH); 1598.52 (stretching, -C=N-); 1497.06 and 1326.15 (bending, -NO_2 groups); 1445.75 (stretching, C=C); 1267.04–1041.86 (stretching, C-N); 719.97 (-C-S-C-) (Table 1). **^{1}H-NMR (300 MHz, DMSO-d_6, δ/ppm):** 7.26–8.93 (16H, Aromatic H); 10.75 (1H, -NH) (see Table 2 for details). **Elemental analysis:** (% calculated/found) for $C_{29}H_{18}N_6O_2S$ (Mw: 514.55) C: 67.69/67.95; H: 3.53/3.67; N:16.33/16.65. **LC-MS/MS (ESI–m/z)[M-1]$^+$:** Calculated/found: 514.55/513.05.

5-(4-(1H-phenanthro[9,10-d]imidazol-2-yl)phenyl)-3-nitrophenyl-1,3,4-thiadiazol-2-amine) (PHN1b)

Light brown powder and purified in DMSO-water. Yield: (88%), melting point (mp): 220 ºC; **ATR-IR (ν_{maks}, cm^{-1}):** 3186.47 (stretching, -NH); 3076.11, 2995.21 (Aromatic C-H); 1651.17 (bending, -NH); 1607.12 (stretching, -C=N-); 1528.22 and 1340.70 (bending, -NO_2 groups); 1426.80 (stretching, C=C); 1340.70–1083.12 (stretching, C-N); 711.61 (-C-S-C-). **^{1}H-NMR (300 MHz, DMSO-$d6$, δ/ppm):** 7.60–8.90 (16 H, Aromatic H); 8.73 (1H, -NH) (see Table 2 for details). **Elemental analysis:** (% calculated/found) for $C_{29}H_{18}N_6O_2S$ (Mw: 514.55) C: 67.69/67.10; H: 3.53/3.49; N:16.33/16.41. **LC-MS/MS (ESI–m/z) [M-1]$^+$:** Calculated/found: 514.55/513.05.

Table 1 FT-IR values for compounds (cm^{-1})

Compounds	$\upsilon_{(NH)}$	$\upsilon_{C-H\ (Aromatic)}$	$\upsilon_{C-H\ (Aliphatic)}$	$\upsilon_{C=C}$	υ_{C-O}	$\upsilon_{(C=N)}$	$\upsilon_{(NO_2)}$	$\upsilon_{(C-Cl)}$	υ_{C-S-C}
PHN1a	3351.56 3248.71	3056.90	-	1445.75	-	1598.52	1497.06 1326.15	-	719.97
PHN1b	3186.47	3076.11 2995.21	-	1426.80	-	1607.12	1528.22 1340.70	-	711.61
PHN1c	3346.27 3201.52 3153.11	3045.40 2989.56	-	1494.14		1605.44	1568.32 1376.80	-	718.99
PHN1d	3335.99 3180.49	3052.35 3000.65	2904.61 2832.49	1464.10	1102.28 1018.28	1602.89 1534.64	-	-	678.62
PHN1e	3240.90 3130.82	3055.06 3001.04	2830.99	1489.31	1094.65 1039.29	1603.73	-	-	684.82
PHN1f	3130.82	3061.81 3021.92	2916.59 2848.86	1447.15	1074.26 1026.98	1604.58 1554.54	-	-	689.04
PHN1g	3182.89	3057.71 2992.13	-	1433.76	-	1604.59 1529.68	-	1093.85	711.49
PHN1h	3168.86	3056.82 2989.03	-	1497.81 1464.21	-	1594.58 1529.34	-	1084.89	708.35
PHN1i	3358.09 3229.11 3174.98	3046.68 2993.55	-	1492.63	-	1606.50 1548.60	-	1088.85	681.24
PHN1j	3172.92	2981.92	2926.64 2851.42	1491.63	-	1609.43 1543.50	-	-	690.41
PHN1k	3181.68 3129.07	2995.00	-	1491.14	-	1603.86 1557.27	-	-	705.97
PHN1l	3280.14	3047.90 2976.34	2862.52	1463.49	-	1604.15	-	-	706.57
PHN1m	3100.90	3053.02 2982.97	2868.45	1464.80	-	1605.12 1554.07	-	-	710.42
PHN1n	3298.84 3177.34	3044.76 2975.82	2867.93 2815.03	1490.71	-	1607.50 1553.38	-	-	706.59
PHN1o	3144.96	3054.08	2923.05 2862.62	1464.22	-	1606.77 1527.33	-	-	707.62

Table 2 ^{1}H-NMR data of the all compounds (δ, ppm, in DMSO-d_6)

Comp	Aromatic	-NH	-substituted groups
PHN1a	8.87 (t, *J* = *8.6 Hz*, 2H), 8.61 (t, *8.3 Hz*, 2H), 8.49 (d, *J* = *6.8 Hz*, 1H), 8.45 (d, *J* = *8.1 Hz*, 1H), 8.27 (d, *J* = *6.7 Hz*, 1H), 8.21 (d, *J* = *8.1 Hz*, 1H), 8.11 (t, *J* = *8.5 Hz*, 2H), 7.77 (t, *J* = *14.0 Hz*, 3H), 7.66 (q, *J* = *7.3 Hz*, 2H), 7.29 (t, *J* = *7.8 Hz*, 1H)	10.76 (s, 1H)	-
PHN1b	8.86 (t, *J* = *8.9 Hz*, 2H), 8.62 (d, *7.6 Hz*, 2H), 8.53 (t, *J* = *8.0 Hz*, 2H), 8.27 (d, *J* = *8.1 Hz*, 2H), 8.22 (d, *J* = *8.1 Hz*, 1H), 8.08 (d, *J* = *7.6 Hz*, 1H), 7.82- 7.59 (m, 6H)	8.73 (s, 1H)	-
PHN1c	8.87 (d, *J* = *7.8 Hz*, 2H), 8.60 (d, *7.8 Hz*, 2H), 8.46 (d, *J* = *8.1 Hz*, 2H), 8.28 (d, *J* = *8.8 Hz*, 2H), 8.14 (d, *J* = *8.1 Hz*, 2H), 7.90 (d, *J* = *8.8 Hz*, 2H), 7.77 (t, *J* = *7.3 Hz*, 2H)	11.37 (s, 1H)	-
PHN1d	8.88 (d, *J* = *8.1 Hz*, 2H), 8.67 (d, *J* = *7.9 Hz*, 2H), 8.48 (d, *J* = *7.8 Hz*, 2H), 8.36 (d, *J* = *7.6 Hz*, 1H), 8.10 (d, *J* = *7.9 Hz*, 2H), 7.78 (t, *J* = *7.1 Hz,* 2H), 7.69 (t, *J* = *7.2 Hz*, 2H), 7.04 (t, *J* = *28.0, 7.5 Hz*, 3H)	10.04 (s, 1H)	3.90 (s, 1H) **(-OCH_3)**
PHN1e	8.92 (d, *J* = *8.3 Hz*, 2H), 8.70 (d, *J* = *7.8 Hz*, 2H), 8.51 (d, *J* = *7.8 Hz*, 2H), 8.16 (d, *J* = *7.9 Hz*, 2H), 7.81 (t, *J* = *7.3 Hz*, 2H), 7.73 (t, *J* = *7.6 Hz,* 2H), 7.41 (s, 1H), 7.29 (t, *J* = *8.0 Hz*, 1H), 7.17 (d, *J* = *8.2 Hz*, 1H), 6.64 (d, *J* = *7.8 Hz*, 1H)	10.74 (s, 1H)	3.79 (s, 1H) **(-OCH_3)**
PHN1f	8.89 (d, *J* = *8.2 Hz*, 2H), 8.64 (d, *J* = *7.6 Hz*, 2H), 8.47 (d, *J* = *8.0 Hz*, 2H), 8.10 (d, *J* = *8.1 Hz*, 2H), 7.79 (t, *J* = *7.2 Hz*, 2H), 7.70 (t, *J* = *7.5 Hz,* 2H), 7.59 (d, *J* = *8.6 Hz*, 2H), 6.69 (d, *J* = *8.5 Hz*, 2H)	10.38 (s, 1H)	3.78 (s, 1H) **(-OCH_3)**
PHN1g	8.90 (t, *J* = *7.9 Hz*, 2H), 8.71 (d, *J* = *7.5 Hz*, 2H), 8.63 (d, *J* = *7.7 Hz*, 1H), 8.57 (d, *J* = *7.6 Hz*, 1H), 8.54–8.47 (m, 1H), 8.35–8.27 (m, 2H), 8.15 (d, *J* = *7.9 Hz*, 1H), 8.03 (d, *J* = *7.4 Hz*, 1H), 7.84–7.68 (m, 6H), 7.61 (d, *J* = *7.7 Hz*, 1H), 7.55 (d, *J* = *7.9 Hz*, 1H)	10.21 (s, 1H)	-
PHN1h	8.89 (d, *J* = *8.6 Hz*, 2H), 8.61 (d, *J* = *7.8 Hz*, 2H), 8.46 (d, *J* = *8.4 Hz*, 2H), 8.13 (d, *J* = *8.2 Hz*, 2H), 7.97 (s, 1H), 7.78 (t, *J* = *7.6 Hz*, 2H), 7.68 (t, *J* = *7.6 Hz,* 2H), 7.51 (d, *J* = *7.1 Hz*, 1H), 7.41 (t, *J* = *8.0 Hz*, 1H), 7.10 (d, *J* = *7.8 Hz*, 1H)	10.88 (s, 1H)	-
PHN1i	8.91 (d, *J* = *8.2 Hz*, 2H), 8.66 (d, *J* = *7.9 Hz*, 2H), 8.49 (d, *J* = *7.6 Hz*, 2H), 8.15 (d, *J* = *7.9 Hz*, 2H), 7.80 (t, *J* = *7.1 Hz*, 2H), 7.72 (dd, *J* = *13.2, 7.7 Hz,* 4H), 7.45 (d, *J* = *8.5 Hz*, 2H)	10.84 (s, 1H)	-
PHN1j	8.90 (d, *J* = *8.2 Hz,* 2H), 8.64 (d, *J* = *7.7 Hz* 2H), 8.43 (d, *J* = 8.1 Hz, 1H), 8.18 (d, *J* = *7.8 Hz,* 1H), 8.10 (d, *J* = *7.2 Hz*, 1H), 7.78 (t, *J* = *7.4 Hz*, 2H), 7.69 (t, *J* = *7.5 Hz*, 2H)	-	2.04 (d, *J* = *9.0 Hz*, 2H); 1.74 (d, 2H); 1.60 (d, *J* = *10.7 Hz*, 1H); 1.44- 1.07 (m, 5H); **(-aliphatic groups)**
PHN1k	8.90 (t, *J* = *8.9 Hz*, 2H), 8.68–8.60 (m, 1H), 8.56 (dd, *J* = *18.2, 7.6 Hz*, 2H), 8.46 (d, *J* = *7.8 Hz*, 1H), 8.31 (d, *J* = *7.8 Hz*, 1H), 8.19 (dd, *J* = *21.3, 12.6 Hz,* 2H), 7.83- 7.74 (m, 2H), 7.70 (d, *J* = *7.6 Hz*, 2H), 7.64 (d, *J* = *6.5 Hz*, 1H), 7.53 (d, *J* = *7.5 Hz*, 1H), 7.46 (t, *J* = *7.5 Hz*, 1H), 7.44- 7.28 (m, 2H)	-	-
PHN1l	8.89 (d, *J* = *7.6 Hz*, 2H), 8.72 (d, *J* = *7.5 Hz*, 2H), 8.68 (d, *J* = *7.7 Hz*, 1H),8.50 (d, J = 7.4 Hz, 2H), 8.17 (d, *J* = *13.5, 8.3 Hz*, 2H), 8.09 (d, *J* = *8.0 Hz,* 1H), 7.78 (d, J = 7.3 Hz, 2H), 7.71 (t, *J* = *7.5 Hz*, 2H), 7.30–7.14 (m, 2H)	7.60 (s, 1H)	2.52 (dd, *J* = *9.7, 3.6 Hz*, 3H) 1.17 (t, *J* = *7.5 Hz*, 2H) **(-aliphatic groups)**
PHN1m	8.92 (t, 2H), 8.78 (d, *J* = *7.5 Hz*, 1H), 8.72 (d, *J* = *7.7 Hz*, 1H), 8.53 (d, *J* = *6.3 Hz*, 2H), 8.21 (d, *J* = *8.1 Hz*, 1H), 8.08 (d, *J* = *8.3 Hz,* 1H), 7.91–7.63 (m, 5H)	-	3.00 (s, 1H) **(-aliphatic groups)**
PHN1n	8.92 (t, *J* = *6.5 Hz,* 2H), 8.80 (d, *J* = *7.8 Hz* 1H), 8.74 (d, *J* = 7.7 Hz, 1H), 8.55 (dd, *J* = *8.1*, 5.8 Hz, 2H), 8.08 (d, *J* = *8.4 Hz*, 1H), 7.77 (td, *J* = *15.0, 7.6 Hz*, 5H)	-	3.40 (dd, *J* = *14.4, 7.2 Hz*, 2H) 1.25 (t, *J* = *7.2 Hz*, 3H) **(-aliphatic groups)**
PHN1o	8.92 (t, 2H), 8.83 (d, *J* = *7.7 Hz*, 1H), 8.76 (d, *J* = *7.9 Hz*, 2H), 8.58 (t, *J* = *7.6 Hz*, 2H), 8.21 (d, *J* = *8.4 Hz*, 2H), 8.07 (d, *J* = *8.4 Hz,* 1H), 7.86- 7.70 (m, 5H), 7.43- 7.23 (m, 3H)	7.32 (s, 1H)	3.62 (m, 2H), 2.97 (dd, *J* = *13.0, 5.6 Hz*, 2H) **(-aliphatic groups)**

5-(4-(1H-phenanthro[9,10-d]imidazol-2-yl)phenyl)-4-nitrophenyl-1,3,4-thiadiazol-2-amine) (PHN1c)

Yellow powder and purified in DMSO-water. Yield: (81%), melting point (mp): 290 °C; **ATR-IR (ν_{maks}, cm^{-1}):** 3346.27, 3201.52 and 3153.11 (stretching, -NH); 3045.40, 2989.56 (Aromatic C-H); 1649.29 (bending, -NH); 1605.44 (stretching, -C = N-); 1568.32 and 1376.80 (bending, -NO_2 groups); 1494.14 (stretching, C = C); 1333.58–1020.58 (stretching, C-N); 718.99 (-C-S-C-). **^{1}H-NMR (300 MHz, DMSO-*d6*, δ/ppm):** 7.62–8.90 (16 H, Aromatic H); 11.37 (1H, -NH) (see Table 2 for details). **Elemental analysis:** (% calculated/found) for $C_{29}H_{18}N_6O_2S$ (Mw: 514.55) C: 67.69/67.57; H: 3.53/3.50; N:16.33/16.55. **LCMS-MS (ESI–m/z) $[M+1]^+$:** Calculated/found: 514.55/515.05.

5-(4-(1H-phenanthro[9,10-d]imidazol-2-yl)phenyl)-2-methoxyphenyl-1,3,4-thiadiazol-2-amine) (PHN1d)

Greenish brown powder and purified in DMSO-water. Yield: (89%), melting point (mp): 294 °C; **ATR-IR (ν_{maks}, cm^{-1}):** 3335.99 and 3180.49 (stretching, -NH); 3052.35, 3000.65 (aromatic C-H); 2904.61, 2832.49 (aliphatic C-H); 1650.95 (bending, -NH); 1602.89, 15,334.64 (stretching, -C = N-); 1018.28 (bending, -OCH_3 groups); 1464.10 (stretching, C = C); 678.62 (-C-S-C-). **^{1}H-NMR (300 MHz, DMSO-d_6, δ/ppm):** 6.98–8.92 (16 H, Aromatic H); 10.02 (1H, -NH); 3.87 (3H, OCH_3) (see Table 2 for details). **Elemental analysis:** (% calculated/found) for $C_{30}H_{21}N_5OS$ (Mw: 499.58) C: 72.12/72.52; H: 4.24/4.41; N:14.02/14.58. **LC-MS/MS (ESI–m/z) $[M+1]^+$:** Calculated/found: 499.58/500.05.

5-(4-(1H-phenanthro[9,10-d]imidazol-2-yl)phenyl)-3-methoxyphenyl-1,3,4-thiadiazol-2-amine) (PHN1e)

Green powder and purified in DMSO-water. Yield: (85%), melting point (mp): 300 °C; **ATR-IR (ν_{maks}, cm^{-1}):** 3240.90 and 3130.82 (stretching, -NH); 3055.06, 3001.04 (aromatic C-H); 2830.99 (aliphatic C-H); 1648.97 (bending, -NH); 1603.73 (stretching, -C = N-); 1039.29 (bending, -OCH_3 groups); 1489.31 (stretching, C = C); 684.82 (-C-S-C-). **^{1}H-NMR (300 MHz, DMSO-*d6*, δ/ppm):** 6.91–8.96 (16 H, Aromatic H); 10.02 (1 H, -NH); 3.81 (3 H, OCH_3) (see Table 2 for details). **Elemental analysis:** (% calculated/found) for $C_{30}H_{21}N_5OS$ (Mw: 499.58) C: 72.12/72.36; H: 4.24/4.23; N:14.02/13.75. **LC-MS/MS (ESI–m/z) $[M+1]^+$:** Calculated/found: 499.58/500.05.

5-(4-(1H-phenanthro[9,10-d]imidazol-2-yl)phenyl)-4-methoxyphenyl-1,3,4-thiadiazol-2-amine) (PHN1f)

Greenish yellow and purified in DMSO-water. Yield: (77%), melting point (mp): 282 °C; **ATR-IR (ν_{maks}, cm^{-1}):** 3130.82 (stretching, -NH); 3061.81 and 3021.92 (aromatic C-H); 2916.59 and 2848.86 (aliphatic C-H); 1651.94 (bending, -NH); 1604.58 and 1554.54 (stretching, -C = N-); 1026.98 (bending, -OCH_3 groups); 1497.81 and 1447.15 (stretching, C = C); 689.04 (-C-S-C-). **^{1}H-NMR (300 MHz, DMSO-d_6, δ/ppm):** 6.95–8.93 (16H, Aromatic H); 10.36 (1H, -NH); 3.76 (3H, OCH_3) (see Table 2 for details). **Elemental analysis:** (% calculated/found) for $C_{30}H_{21}N_5OS$ (Mw: 499.58) C: 72.12/72.14; H: 4.24/4.44; N:14.02/14.14. **LC-MS/MS (ESI–m/z) $[M+1]^+$:** Calculated/found: 499.58/500.05.

5-(4-(1H-phenanthro[9,10-d]imidazol-2-yl)phenyl)-2-chlorophenyl-1,3,4-thiadiazol-2-amine) (PHN1g)

Dark brown powder and purified in DMSO-water. Yield: (83%), melting point (mp): 291 °C; **ATR-IR (ν_{maks}, cm^{-1}):** 3182.89 (stretching, -NH); 3057.71 and 2992.13 (aromatic C-H); 1653.91 (bending, -NH); 1604.59 and 1529.68 (stretching, -C = N-); 1433.76 (stretching, C = C); 1093.85 (stretching C–Cl); 711.49 (-C-S-C-). **^{1}H-NMR (300 MHz, DMSO-d_6, δ/ppm):** 7.40–8.95 (16 H, Aromatic H) (see Table 2 for details). **Elemental analysis:** (% calculated/found) for $C_{29}H_{18}ClN_5S$ (Mw: 504.00) C: 69.11/69.38; H: 3.60/3.21; N:13.90/14.01. **LC-MS/MS (ESI–m/z) $[M]^+$:** Calculated/found: 504.00/504.0

5-(4-(1H-phenanthro[9,10-d]imidazol-2-yl)phenyl)-3-chlorophenyl-1,3,4-thiadiazol-2-amine) (PHN1h)

Dark brown powder and purified in DMSO-water. Yield: (81%), melting point (mp): 310 °C; **ATR-IR (ν_{maks}, cm^{-1}):** 3168.86 (stretching, -NH); 3056.82 and 2989.03 (aromatic C-H); 1650.93 (bending, -NH); 1594.58 and 1529.34 (stretching, -C = N-); 1497.81 and 1464.21 (stretching, C = C); 1084.89 (stretching C–Cl); 708.35 (-C-S-C-). **^{1}H-NMR (300 MHz, DMSO-d_6, δ/ppm):** 7.04–8.95 (16H, Aromatic H); 10.87 (1H, -NH) (see Table 2 for details). **Elemental analysis:** (% calculated/found) for $C_{29}H_{18}ClN_5S$ (Mw: 504.00) C: 69.11/69.94; H: 3.60/3.91; N:13.90/13.64. **LC-MS/MS (ESI–m/z) $[M]^+$:** Calculated/found: 504.00/504.05.

5-(4-(1H-phenanthro[9,10-d]imidazol-2-yl)phenyl)-4-chlorophenyl-1,3,4-thiadiazol-2-amine) (PHN1i)

Greenish yellow powder and purified in DMSO-water. Yield: (87%), melting point (mp): 280 °C; **ATR-IR (ν_{maks}, cm^{-1}):** 3358.09, 3229.11 and 3174.98 (stretching, -NH); 3046.68

and 2993.55 (aromatic C-H); 1651.37 (bending, -NH); 1606.50 and 1548.60 (stretching, -C=N-); 1492.63 (stretching, C=C); 1088.85 (stretching C–Cl); 681.24 (-C-S-C-). **^{1}H-NMR (300 MHz, DMSO-d_6, δ/ppm):** 7.41–8.94 (16H, Aromatic H); 10.83 (1H, -NH) (see Table 2 for details). **Elemental analysis:** (% calculated/found) for $C_{29}H_{18}ClN_5S$ (Mw: 504.00) C: 69.11/69.25; H: 3.60/3.60; N:13.90/13.13. **LC-MS/MS (ESI–m/z) [M]$^+$:** Calculated/found: 504.00/504.00.

5-(4-(1H-phenanthro[9,10-d]imidazol-2-yl)phenyl)-N-cyclohexyl-1,3,4-thiadiazol-2-amine) (PHN1j)

Yellow powder and purified in DMSO-water. Yield: (83%), melting point (mp): 245 ºC; **ATR-IR (ν_{maks}, cm^{-1}):** 3172.92 (stretching, -NH); 2981.92 (aromatic C-H); 2926.64 and 2851.42 (aliphatic C-H); 1651.73 (bending, -NH); 1609.43 and 1543.50 (stretching, -C=N-); 1491.63 (stretching, C=C); 1093.17 and 978.76 (bending, C-H in cyclohexyl); 690.41 (-C-S-C-). **^{1}H-NMR (300 MHz, DMSO-*d6*, δ/ppm):** 7.63–8.94 (12 H, Aromatic H); 2.12–1.01 (10H, -cyclohexyl) (see Table 2 for details). **Elemental analysis:** (%calculated/found) for $C_{29}H_{25}N_5S$ (Mw: 475.60) C: 73.23/72.47; H: 5.30/5.31; N:14.73/14.21. **LC-MS/MS (ESI–m/z) [M + 1]$^+$:** Calculated/found: 475.60/476.05.

5-(4-(1H-phenanthro[9,10-d]imidazol-2-yl)phenyl)-N-phenyl-1,3,4-thiadiazol-2-amine) (PHN1k)

Brown powder and purified in DMSO-water. Yield: (89%), melting point (mp): 235 ºC **ATR-IR (ν_{maks}, cm^{-1}):** 3181.68 and 3129.07 (stretching, -NH); 2995.00 (aromatic C-H); 1655.89 (bending, -NH); 1603.86 and 1557.27 (stretching, -C=N-); 1491.14 (stretching, C=C); 705.97 (-C-S-C-). **^{1}H-NMR (300 MHz, DMSO-d_6, δ/ppm):** 7.34–8.93 (17 H, Aromatic H) (see Table 2 for details). **Elemental analysis:** (%calculated/found) for $C_{29}H_{19}N_5S$ (Mw: 469.55) C: 74.18/74.55; H: 4.08/4.16; N:14.91/14.62. **LC-MS/MS (ESI–m/z) [M + 1]$^+$:** Calculated/found: 469.55/470.00.

5-(4-(1H-phenanthro[9,10-d]imidazol-2-yl)phenyl)-N-ethenephenyl-1,3,4-thiadiazol-2-amine) (PHN1l)

Light brown powder and purified in DMSO-water. Yield: (75%), melting point (mp): 300 ºC; **ATR-IR (ν_{maks}, cm^{-1}):** 3280.14 (stretching, -NH); 3047.90 and 2976.34 (aromatic C-H); 2862.52 (aliphatic C-H); 1646.86 (bending, -NH); 1604.15 (stretching, -C=N-); 1463.49 (stretching, C=C); 706.57 (-C-S-C-). **^{1}H-NMR (300 MHz, DMSO-d_6, δ/ppm):** 7.14–8.89 (16H, Aromatic H); 2.96 (2H, -CH_2); 1.18 (3H, -CH_3) (see Table 2 for details). **Elemental analysis:** (%calculated/found) for $C_{31}H_{23}N_5S$ (Mw: 497.61) C: 74.82/74.18; H: 4.66/5.03; N:14.07/14.15. **LC-MS/MS (ESI–m/z) [M + 1]$^+$:** Calculated/found: 497.61/498.10.

5-(4-(1H-phenanthro[9,10-d]imidazol-2-yl)phenyl)-N-methyl-1,3,4-thiadiazol-2-amine) (PHN1m)

Brown powder and purified in DMSO-water. Yield: (91%), melting point (mp): 300 ºC; **ATR-IR (ν_{maks}, cm^{-1}):** 3100.90 (stretching, -NH); 3053.02 and 2982.97 (aromatic C-H); 2868.45 (aliphatic C-H); 1645.70 (bending, -NH); 1605.12 and 1554.07 (stretching, -C=N-); 1464.80 (stretching, C=C); 710.42 (-C-S-C-). **^{1}H-NMR (300 MHz, DMSO-d_6, δ/ppm):** 7.61–8.98 (12 H, Aromatic H); 2.98 (3 H, -CH_3) (see Table 2 for details). **Elemental analysis:** (%calculated/found) for $C_{24}H_{17}N_5S$ (Mw: 407.05) C: 70.74/69.24; H: 4.21/4.73; N:17.19/17.04. **LC-MS/MS (ESI–m/z) [M + 1]$^+$:** Calculated/found: 407.49/408.05.

5-(4-(1H-phenanthro[9,10-d]imidazol-2-yl)phenyl)-N-ethyl-1,3,4-thiadiazol-2-amine) (PHN1n)

Light brown powder and purified in DMSO-water. Yield: (89%), melting point (mp): 280 ºC; **ATR-IR (ν_{maks}, cm^{-1}):** 3298.84 and 3177.34 (stretching, -NH); 3044.76 and 2975.82 (aromatic C-H); 2867.93 and 2815.03 (aliphatic, C-H); 1645.16 (bending, -NH); 1607.50 and 1553.38 (stretching, -C=N-); 1490.71 (stretching, C=C); 706.59 (-C-S-C-). **^{1}H-NMR (300 MHz, DMSO-d_6, δ/ppm):** 7.70–8.97 (12 H, Aromatic H); 3.41 (2 H,-CH_2); 1.40 (3 H, -CH_3) (see Table 2 for details). **Elemental analysis:** (%calculated/found) for $C_{25}H_{19}N_5S$ (Mw: 421.51) C: 71.23/69.84; H: 4.54/4.548; N:16.61/16.01. **LC-MS/MS (ESI–m/z) [M + 1]$^+$:** Calculated/found: 421.51/422.05.

5-(4-(1H-phenanthro[9,10-d]imidazol-2-yl)phenyl)-N-ethenephenyl-1,3,4-thiadiazol-2-amine) (PHN1o)

Light yellow powder and purified in DMSO-water. Yield: (86%), melting point (mp): 249 ºC; **ATR-IR (ν_{maks}, cm^{-1}):** 3144.96 (stretching, -NH); 3054.08 (aromatic C-H); 2923.05 and 2862.62 (aliphatic C-H); 1656.34 (bending, -NH); 1606.77 and 1527.33 (stretching, -C=N-); 1464.22–1455.42 (stretching, C=C); 707.62 (-C-S-C-). **^{1}H-NMR (300 MHz, DMSO-d_6, δ/ppm):** 7.21–8.90 (17H, Aromatic H); 3.62 (2H, -CH_2); 2.97 (2H, -CH_2) (see Table 2 for details). **Elemental analysis:** (%calculated/found) for $C_{31}H_{23}N_5S$ (Mw: 497.61) C: 74.82/75.37; H: 4.66/4.81; N:14.07/14.32. **LC-MS/MS (ESI–m/z) [M + 1]$^+$:** Calculated/found: 497.61/498.10 [28].

Results and Discussion

Design, Synthesis and Characterization

The synthetic route that were utilized for synthesis of the phenanthroimidazole-thiadiazole hybrids were summarized in Scheme 1. First step in the route is the formation of the phenanthroimidazole ring using procedure

of the condensation reaction [8, 34]. In the last step, fifteen new compounds were synthesized with aromatic and aliphatic substituted also electron donating and electron withdrawing in the *o*, *m*- and *p*- positions of these groups. Fifteen aromatic and aliphatic substituted compounds were successfully obtained in 77–91% yields. The new fluorescent phenanthroimidazole-thiadiazole derivatives structure is given in Fig. 1. The structures

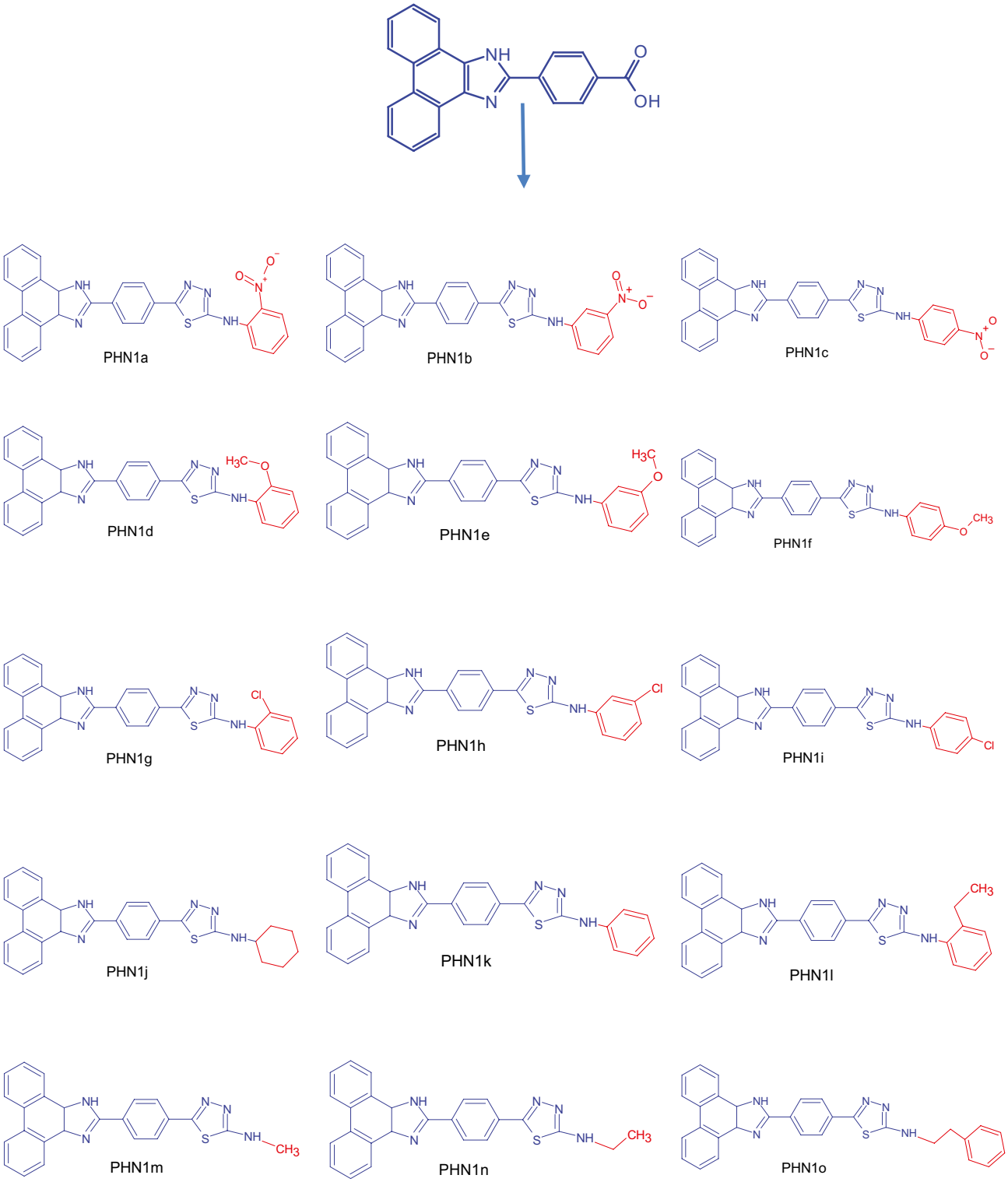

Fig. 1 Structure of the new fluorescent phenanthroimidazole-thiadiazole derivatives

of new phenanthroimidazole-thiadiazole hybrid derivatives structure were confirmed by the assistance of ATR-IR, ^{1}H-NMR, mass analysis and elemental analysis. The infrared vibration spectra of the compounds are given in supplementary information. In the ATR-IR spectra of compounds; peaks of carbonyl group (1722.68 cm^{-1}) and hydroxyl group (3057.78 cm^{-1}) vibrations in the starting reagent were not observed. Instead of this peaks, in the ATR-IR spectra of the compound, vibrations of groups such as -NH, NO_2, O-C, C–Cl, C-S-C and different peaks appeared according to different substitution groups.

When the ATR-IR spectra of the compounds are analyzed, the bands resulting from -NH stretching vibrations were seen in the range of 3358.09 – 3100.90 cm^{-1}. While the peaks seen between 3061.90 cm^{-1}–2981.92 cm^{-1} were seen to be the peaks caused by aromatic C-H stretching, aliphatic C-H stretching vibrations are seen in the range of 2926.64 cm^{-1}–2815.03 cm^{-1}. The peaks observed in the range of 1607.50 cm^{-1}–1527.33 cm^{-1} were observed to correspond to the C = N stretching vibrations in the thiadiazole rings. The stretching vibrations of the C = C group were observed in the range of 1494.21 cm^{-1}–1426.80 cm^{-1}. The C-S-C group vibrations in the thiadiazole ring were detected at the range of 719–97 cm^{-1}–681.24 cm^{-1} (Table 1).

When the ^{1}H-NMR spectra of the compounds were examined, the single peak at 3.90, 3.79 and 3.78 ppm belongs to the $–OCH_3$ protons in the methoxy group in the phenyl ring (compound **PHN1d**, **PHN1e** and **PHN1f**).

It was observed the aliphatic protons in the compounds **PHN1j**, **PHN1l**, **PHN1m**, **PHN1n** and **PHN1o** in the range of 1.07- 3.62 ppm. These aliphatic protons which belong to $–CH_3$ and $–CH_2$ protons were seen as the multiple, triplet, doublet and singlet.

In addition, the $–CH_2$ protons in cyclohexyl groups in the **PHN1j** compound were observed as multiplet and doublet between 1.07–2.04 ppm. -NH protons were detected at the range of 7.32–11.37 ppm as a singlet peak. The peaks of aromatic protons in phenanthrene structure and other aromatic protons were seen as doublet and triplet at the range of 6.04–8.92 ppm. (All ^{1}H-NMR spectra are presented in detail in the Supplementary Information file S16–S30).

Photophysical Properties

The photophysical studies of new phenanthroimidazole-thiadiazole hybrids which obtained from different substituted groups, aromatic and aliphatic structure were performed using absorption and fluorescence techniques. The photophysical properties of the compounds were investigated by binding electron withdrawing and electron donating groups to the molecule at *o-, m- and p-* positions in cause of changing the intramolecular charge transfer.

The photophysical studies were made in DMSO at room temperature (1×10^{-5} M). Maximum absorption and emission wavelengths (λ_{max}), Stokes' shifts, molar extinction coefficients (ε), singlet energy levels (Es), quantum yield (ϕ_f) and lifetime (τ) of compounds are presented (Table 3). The normalized UV–Vis absorption and fluorescence emission spectra of the synthesized derivatives in DMSO (1×10^{-5} M) are presented in Fig. 2.

Table 3 Photophysical properties data for all compounds in DMSO 1×10^{-5} M (λ_{max}, Stokes' shift, molar extinction efficient, singlet energy levels, quantum yield and lifetime)

Compounds	Max. Absorbance (λ_{max})	Max. Emission (λ_{max})	Stokes' Shift (λ)	Molar Extinction Efficient (L/mol·cm)	Singlet Energy Levels (kcal/mol)	Quantum Yield	Lifetime (ns)
PHN1a	378	438	60	42,800	75.98	0.103	1.617
PHN1b	373	431	58	33,000	76.99	0.262	2.053
PHN1c	395	456	61	61,100	72.70	0.016	2.063
PHN1d	382	445	63	37,000	75.18	0.131	1.810
PHN1e	383	449	66	66,900	74.98	0.46	1.606
PHN1f	381	443	62	32,400	75.38	0.12	1.948
PHN1g	378	463	85	34,800	75.98	0.16	1.847
PHN1h	381	455	74	59,900	75.18	0.72	1.813
PHN1i	382	453	71	59,900	75.18	0.56	1.619
PHN1j	377	440	63	47,100	76.17	0.68	1.889
PHN1k	373	438	65	16,300	76.99	0.83	2.117
PHN1l	374	441	67	26,700	76.79	0.75	2.170
PHN1m	375	439	64	30,200	76.58	0.86	2.075
PHN1n	376	440	64	37,000	76.38	0.77	2.030
PHN1o	375	437	62	42,000	76.58	0.69	1.783

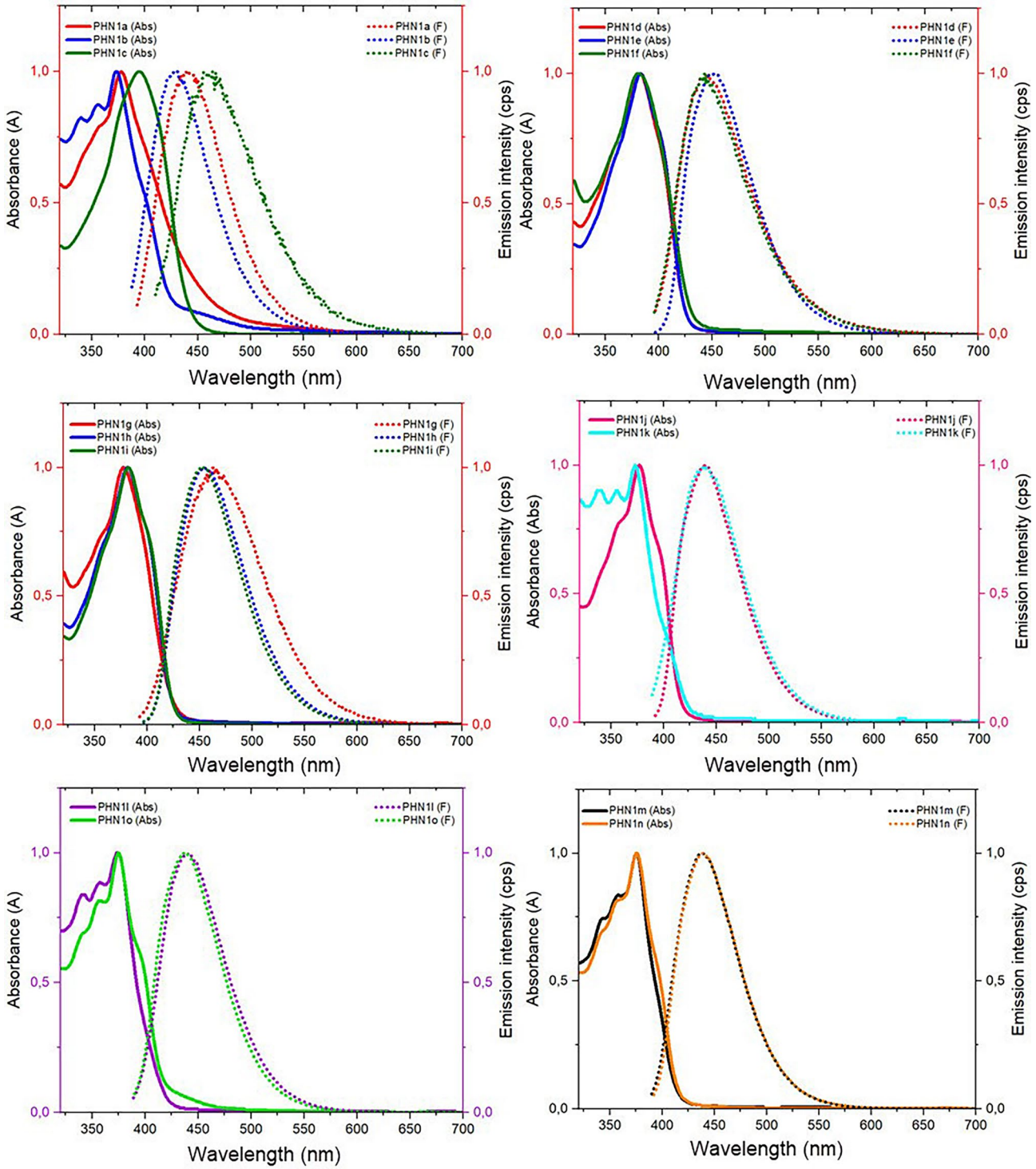

Fig. 2 Normalized absorption and emission steady-state spectra of all compounds in DMSO (1×10^{-5} M)

Steady-state Absorption and Emission Studies

The **PHN1a-o** derivatives exhibited maximum absorption and emission wavelength between 373–395 nm and 431–463 nm. Accordingly, Stokes' shift values were found to be between 58–85 nm (Table 3 and Fig. 2). Difference in the substituent groups of the compounds, showed shifts according to the electronic structure of the substituent in absorption and emission spectra [35]. It was observed that the fluorescence bands of the molecule with -Cl substituents

(**PHN1g, PHN1h** and **PHN1i**) shifted to longer wavelengths compared to other molecules carrying the -OCH_3 and -NO_2 substituents (Table 3). Accordingly, it was found that the highest Stokes' shift values belonged to *-chloro* substituted compounds. It was observed that the lowest Stokes' shift values belonged to the compounds carrying –NO_2 moiety (**PHN1a**, **PHN1b** and **PHN1c**). The nitro groups deactivates the ring, reducing the mobility of electrons [36, 37].

In the -NO_2 group, which is the electron-withdrawing group, a red shift of the para position compound relative to the *-ortho* and *-meta* position was observed in the absorbance and fluorescence spectra. Stokes shift was higher in *para-* substituted compound (**PHN1c**). Accordingly, the *para-* substituted compound (**PHN1c**) has the highest molar absorption coefficient and the lowest singlet energy level.

The -OCH_3 group, which is the electron donating group, has a red shift in the spectra of the *ortho-* and *para-* positions compounds compared to the *meta-* position. The *meta-* substituted compound has the highest stokes shift and molar absorption coefficient. Accordingly, the singlet energy level is the lowest compound.

When the *ortho-*, *meta-* and *para-* positions of -Cl bound compounds are compared, the absorption wavelengths are similar to each other. Accordingly, the singlet energy level was close to each other. When the fluorescence emission spectra were examined, it was seen that the highest wavelength and Stokes shift belonged to the *ortho-* position compound. On the other hand, the molar absorption coefficient of the *meta-* and *para-* substituted compounds was found to the same and *ortho-* substituted compound (**PHN1g**) was found to be the lowest.

The color properties of the compounds in DMSO under daylight and UV lamp is seen in Fig. 3. It has been observed that compounds, which is light yellow in daylight, emits blue under UV lamp. Synthesized compounds are presented deep-blue emission in DMSO at room temperature.

Fluorescence quantum yields and lifetime measurements

-Nitro substituted compounds (**PHN1a, PHN1b** and **PHN1c**), ıt was observed that there was a significant decrease in quantum yields and emission intensities (Table 3 and Fig. 2). Among other components, the *p*-nitro substituted compound (**PHN1c**) has the lowest emission intensity and the lowest quantum yield. Due to the strong electron withdrawing effect of nitro groups bounded to the aromatic ring [38], it was determined that LUMO energy levels were low and nitro groups attached to the fluorophore group with benzene had a fluorescence reducing effect [36, 39]. When the quantum yields of the compounds are examined; ıt was seen that the highest quantum yield belonged to the **PHN1m** compound, and the lowest quantum yield belonged to the -NO_2 derivatives (especially **PHN1c**). The quantum yields of the compounds are respectively **PHN1m** (0.86) > **PHN1k** (0.83) > **PHN1n** (0.77) > **PHN1l** (0.75) > **PHN1h** (0.72) > **PHN1o** (0.69) > **PHN1j** (0.68) > **PHN1i** (0.56) > **PHN1e** (0.46) > **PHN1b** (0.26) > **PHN1g** (0.16) > **PHN1d** (0.12) > **PHN1a** (0.103) > **PHN1c** (0.016). Perylene in cyclohexane ($\Phi f = 0.94$) was used as a reference [30, 31]. The fluorescence quantum yield was determined in the range of 0.016–0.86.

In the presence of electron donating and electron withdrawing groups: When the *ortho-*, *meta-* and *para-* positions were compared among themselves, it was observed that the highest quantum yield belonged to the meta position compounds (**PHN1b, PHN1e, PHN1h**). When the aliphatic and

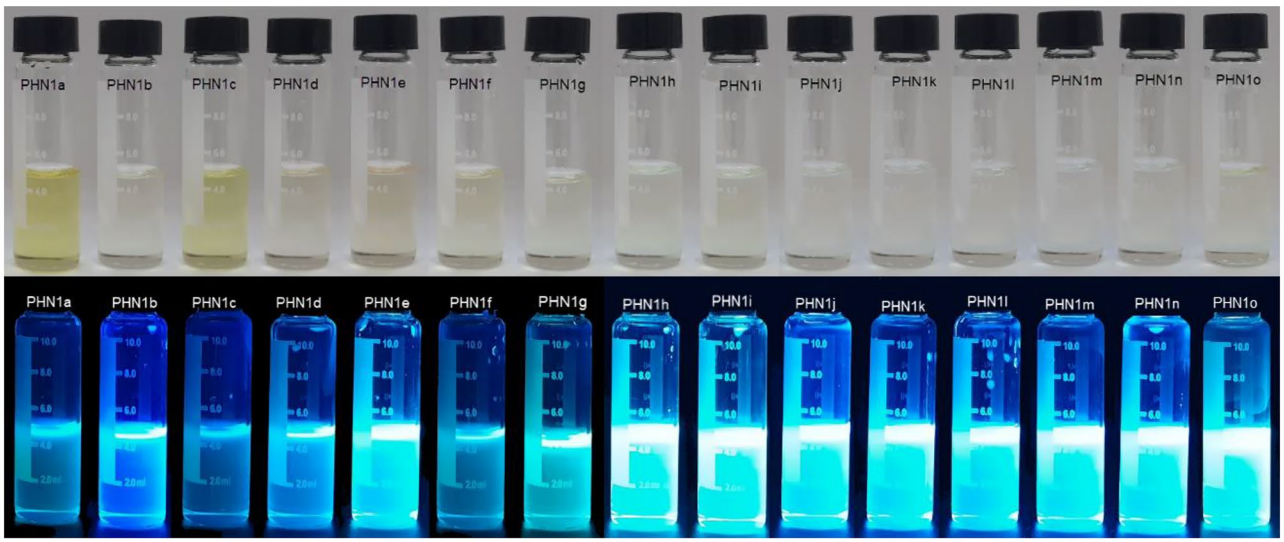

Fig. 3 Images of all compounds in daylight (up) and UV lamp at 365 nm (bottom) in DMSO solutions

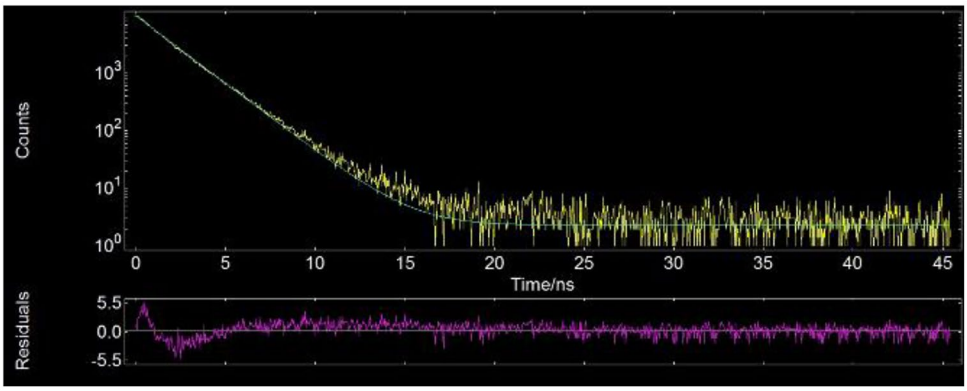

Fig. 4 Fluorescence lifetime decay spectra of compound **PHN1g** in DMSO (λ_{exc} = 378 nm) τ = 1.847 ns (up) The obtained residual graphs (x^2 = 1.870 ns) (bottom)

aromatic groups were compared among themselves, it was observed that the compound with the cyclohexyl (**PHN1j**) had the lowest quantum yield. This result confirms the thesis that the fluorescence quantum efficiency decreases with the decrease in the pi electron system length. In addition, the binding of electron donating and electron withdrawing groups to the structure decreased the quantum yield.

Fluorescence lifetime measurements (τ) were performed by time-resolved fluorescence measurements. Fluorescence lifetimes of the compounds were measured in ambient conditions in DMSO. In Fig. 4 we present time-resolved fluorescence lifetime curve (up), residuals graphs (bottom) of **PHN1g**. All compounds τ values were given Table 4. **PHN1l** (2.170 ns) has the highest lifetime, while **PHN1e** (1.606 ns) has the lowest among other compounds.

The radiative (k_r) and nonradiative (k_{nr}) rate constant values and were determined in this study. The constants k_r and k_{nr} are often calculated by determining the quantum yield and fluorescence lifetime of materials [40, 41]. Fluorescence efficiency is owing to the balance between the radiative and nonradiative rate constants [42]. k_{nr} and k_r calculated by using Eqs. (2) and (3). -*p* nitro substituted **PHN1c** displayed the low quantum yield Φ_f (0.016) and smallest k_r (0.775) among all compounds. The otherwise, **PHN1m** has the highest Φ_f value (0.86), which was the largest k_r (41.445). In addition, **PHN1m** is among the compounds with the largest τ values (2.075 ns). When the *ortho-, meta-* and *para-* positions are evaluated among each series, the highest fluorescence lifetime; It was observed in the para position in the $–NO_2$ and $-OCH_3$ series and in the *ortho-* position in the -Cl series. On the other hand, k_r was found to belong to the highest *meta-* position in all series.

$$K_r = \Phi f/\tau \tag{2}$$

$$K_{nr} = (1 - \Phi f)/\tau \tag{3}$$

Table 4 Radiative and nonradiative rate constants of all compounds in DMSO (2×10^{-4} M)

Compounds	$K_r \times 10^7$ (s^{-1})	$K_{nr} \times 10^7$ (s^{-1})
PHN1a	6.369	55.473
PHN1b	12.761	35.947
PHN1c	0.775	47.697
PHN1d	7.237	48.01
PHN1e	28.642	33.623
PHN1f	6.160	45.174
PHN1g	8.662	45.479
PHN1h	39.713	15.444
PHN1i	34.589	27.177
PHN1j	35.997	16.940
PHN1k	39.206	8.030
PHN1l	34.562	11.520
PHN1m	41.445	6.746
PHN1n	37.931	11.330
PHN1o	38.698	17.386

Aggregation Behaviours

Fluorescent compounds tend to aggregate due to their molecular structure and strong π-electron systems [43]. Aggregation is an important parameter that changes the photophysical properties of organic compounds and aggregation of these compounds is undesirable [44, 45]. In this context, in order to examine the aggregation properties of the phenanthroimidazole derivative compounds, measurements were made in DMSO at different concentrations. For this purpose, the change of UV–Vis spectral measurements at 7 different points in the range of 2.0×10^{-5} M-2.0×10^{-6} M is given in Fig. 5. When the graphs were examined, it was observed that there was no deviation in the correlation graph (between r^2 = 0,9910-0,9995), the compounds did not aggregate in concentration ranges. The UV–Vis spectra of the all compounds in different concentration for aggregation behaviours are given in Supplementary Information (S46–S60).

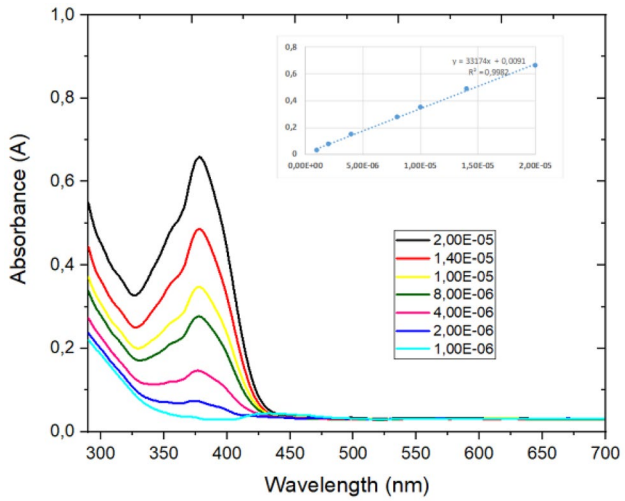

Fig. 5 The UV–Vis spectra of the compound **PHN1g** in different concentration (2.0×10^{-5} M-2.0×10^{-6} M)

Conclusion

In this study, a two-step reaction mechanism was designed and phenanthroimidazole based 1,3,4-thiadiazole hybrid derivatives were synthesized with high fluorescence properties. The framework is derivatized with different substituents (electron donating, electron withdrawing). The photophysical properties of the 15 new compounds obtained were investigated in detail. The quantum yields of compounds in solution found between 1.6% and 86%. Fluorescence lifetime of compounds varied range 1.617–2.170 ns. When the photophysical measurement results were examined, it was clearly seen that the electro-withdrawing and electron-donating groups in the *ortho-, meta- and para-* positions had a significant effect on the fluorescence properties of the compounds. It has been observed that the phenanthroimidazole-thiadiazole derivative compounds are candidates to take their place among the fluorescent organic materials with their strong absorption and emission properties, wide Stokes' shift, high quantum yield and lifetime values. In our previous study, the strong optical and electrochemical properties of *-phenethyl* substituted phenanthroimidazole-thiadiazole derivative were determined and it was revealed that it constitutes a step for optoelectronic device design. With these features, it has proven that can be used in different technologies such as fluorescent laser dyes, OLED technology, solar cells, bioimaging and sensors.

Supplementary Information The online version contains supplementary material available at https://doi.org/10.1007/s10895-022-02916-3.

Acknowledgements We would like to thank the Central Research Laboratories of Kastamonu University for their contributions to our laboratory works.

Author Contributions **Merve Zurnacı:** Synthesis, Investigation, Characterization, Photophysical measurements, Writing–original draft. **İzzet Şener:** Synthesis, Investigation, Characterization, Funding acquisition, Equipment supply, Review & editing**. Mahmut Gür:** Synthesis, Investigation, Characterization, Review & editing. **Nesrin Şener:** Synthesis, Investigation, Characterization, Review & editing.

Funding No funds, grants, or other support was received.

Data Availability ChemDraw, ChemSketch, Origin.

Declarations

Ethics Approval Not applicable.

Consent to Participate Not applicable.

Consent for Publication Not applicable.

Conflicts of Interest There are no conflicts to declare.

References

1. Basabe-Desmonts L, Müller TJJ, Crego-Calama M (2007) Design of fluorescent materials for chemical sensing. Chem Soc Rev 36:993–1017. https://doi.org/10.1039/b609548h
2. Ivanauskaite A, Lygaitis R, Raisys S et al (2017) Structure-property relationship of blue solid state emissive phenanthroimidazole derivatives. Phys Chem Chem Phys 19:16737–16748. https://doi.org/10.1039/c7cp02248d
3. Nayak MK (2012) Synthesis, characterization and optical properties of aryl and diaryl substituted phenanthroimidazoles. J Photochem Photobiol A Chem 241:26–37. https://doi.org/10.1016/j.jphotochem.2012.05.018
4. Ramkumar V, Kannan P (2015) Novel heterocyclic based blue and green emissive materials for opto-electronics. Opt Mater (Amst) 46:314–323. https://doi.org/10.1016/j.optmat.2015.04.038
5. Tang CW, Vanslyke SA (1987) Organic electroluminescent diodes. Appl Phys Lett 51:913–915. https://doi.org/10.1063/1.98799
6. Kula S, Szlapa-Kula A, Kotowicz S et al (2018) Phenanthro[9,10-d]imidazole with thiophene rings toward OLEDs application. Dye Pigment 159:646–654. https://doi.org/10.1016/j.dyepig.2018.07.014
7. Frath D, Massue J, Ulrich G, Ziessel R (2014) Luminescent materials: Locking π-conjugated and heterocyclic ligands with boron(III). Angew Chemie - Int Ed 53:2290–2310. https://doi.org/10.1002/anie.201305554
8. Ferreira RCM, Costa SPG, Gonçalves H et al (2017) Fluorescent phenanthroimidazoles functionalized with heterocyclic spacers: Synthesis, optical chemosensory ability and two-photon absorption (TPA) properties. New J Chem 41:12866–12878. https://doi.org/10.1039/c7nj02113e
9. Martínez Hardigree JF, Katz HE (2014) Through thick and thin: Tuning the threshold voltage in organic field-effect transistors. Acc Chem Res 47:1369–1377. https://doi.org/10.1021/ar5000049
10. Zhang C, Zhu X (2017) Thieno[3,4-b]thiophene-based novel small-molecule optoelectronic materials. Acc Chem Res 50:1342–1350. https://doi.org/10.1021/acs.accounts.7b00050

11. Chen Z, Obaid SN, Lu L (2019) Recent advances in organic optoelectronic devices for biomedical applications. Opt Mater Express 9:3843. https://doi.org/10.1364/ome.9.003843
12. Guo X, Baumgarten M, Müllen K (2013) Designing π-conjugated polymers for organic electronics. Prog Polym Sci 38:1832–1908. https://doi.org/10.1016/j.progpolymsci.2013.09.005
13. Doan PH, Pitter DRG, Kocher A et al (2015) Two-photon spectroscopy as a new sensitive method for determining the dna binding mode of fluorescent nuclear dyes. J Am Chem Soc 137:9198–9201. https://doi.org/10.1021/jacs.5b02674
14. Sun YF, Huang W, Lu CG, Cui YP (2009) The synthesis, two-photon absorption and blue upconversion fluorescence of novel, nitrogen-containing heterocyclic chromophores. Dye Pigment 81:10–17. https://doi.org/10.1016/j.dyepig.2008.08.003
15. Tagare J, Vaidyanathan S (2018) Recent development of phenanthroimidazole-based fluorophores for blue organic light-emitting diodes (OLEDs): an overview. J Mater Chem C 6:10138–10173. https://doi.org/10.1039/C8TC03689F
16. Wang F, Hu J, Cao X et al (2015) A low-cost phenylbenzoimidazole containing electron transport material for efficient green phosphorescent and thermally activated delayed fluorescent OLEDs. J Mater Chem C 3:5533–5540. https://doi.org/10.1039/c5tc00350d
17. Wang Z, Lu P, Chen S et al (2011) Phenanthro[9,10-d]imidazole as a new building block for blue light emitting materials. J Mater Chem 21:5451–5456. https://doi.org/10.1039/c1jm10321k
18. John JC, Shanmugasundaram K, Puthanveedu A et al (2020) Introduction of heterocyclic ring to phenanthroimidazole moiety for efficient blue emitting ionic small molecule LECs. Org Electron 87:105939. https://doi.org/10.1016/j.orgel.2020.105939
19. Hwang SM, Chae JB, Kim C (2018) A phenanthroimidazole-based fluorescent turn-off chemosensor for the selective detection of Cu2+ in aqueous media. Bull Korean Chem Soc 39:925–930. https://doi.org/10.1002/bkcs.11526
20. Chen WC, Yuan Y, Ni SF et al (2017) Highly efficient deep-blue electroluminescence from a charge-transfer emitter with stable donor skeleton. ACS Appl Mater Interfaces 9:7331–7338. https://doi.org/10.1021/acsami.6b14638
21. Liu B, Zhao J, Luo C et al (2016) A novel bipolar phenanthroimidazole derivative host material for highly efficient green and orange-red phosphorescent OLEDs with low efficiency roll-off at high brightness. J Mater Chem C 4:2003–2010. https://doi.org/10.1039/c5tc04393j
22. Chen M, Yuan Y, Zheng J et al (2015) Novel bipolar phenanthroimidazole derivative design for a nondoped deep-blue emitter with high singlet exciton yields. Adv Opt Mater 3:1215–1219. https://doi.org/10.1002/adom.201500258
23. Huang Z, Xiang S, Zhang Q et al (2018) Highly efficient green organic light emitting diodes with phenanthroimidazole-based thermally activated delayed fluorescence emitters. J Mater Chem C 6:2379–2386. https://doi.org/10.1039/c7tc05576e
24. Kula S, Ledwon P, Maroń AM et al (2021) Synthesis, photophysical properties and electroluminescence characterization of 1-phenyl-1H-phenanthro[9,10-d]imidazole derivatives with N-donor substituents. Dye Pigment 192:1–9. https://doi.org/10.1016/j.dyepig.2021.109437
25. Pang H, Skabara PJ, Crouch DJ et al (2007) Structural and electronic effects of 1,3,4-thiadiazole units incorporated into polythiophene chains. Macromolecules 40:6585–6593. https://doi.org/10.1021/ma071242n
26. Tao Y, Xu Q, Lu J, Yang X (2010) The synthesis, electrochemical and fluorescent properties of monomers and polymers containing 2,5-diphenyl-1,3,4-thiadiazole. Dye Pigment 84:153–158. https://doi.org/10.1016/j.dyepig.2009.07.007
27. Şener İ, Şahin Ç, Demir S et al (2020) A combined experimental and computational study of electrochemical and photophysical properties of new benzophenone derivatives functionalized with N-substituted-phenyl-1,3,4-thiadiazole-2-amine. J Mol Struct 1203. https://doi.org/10.1016/j.molstruc.2019.127475
28. Zurnacı M, Ünal F, Demir S et al (2021) Synthesis of a new 1,3,4-thiadiazole-substituted phenanthroimidazole derivative, its growth on glass/ITO as a thin film and analysis of some surface and optoelectronic properties. New J Chem. https://doi.org/10.1039/D1NJ04375G
29. Parker CA, Rees WT (1960) Corrections of fluorescence spectra and the measurement of fluorescence efficiency. Analyst 85:587–600
30. Brouwer AM (2011) Standards for photoluminescence quantum yield measurements in solution (IUPAC technical report). Pure Appl Chem 83:2213–2228. https://doi.org/10.1351/PAC-REP-10-09-31
31. Berlman IB (1971) handbook of fluorescence spectra of aromatic molecules. Second, New York
32. Tapu D, Owens C, Vanderveer D, Gwaltney K (2009) The first phenanthrene-fused imidazol-2-ylidene and its transition-metal complexes. 270–276
33. Ezabadi IR, Camoutsis C, Zoumpoulakis P et al (2008) Sulfonamide-1,2,4-triazole derivatives as antifungal and antibacterial agents: Synthesis, biological evaluation, lipophilicity, and conformational studies. Bioorganic Med Chem 16:1150–1161. https://doi.org/10.1016/j.bmc.2007.10.082
34. Eseola AO, Akogun O, Görls H et al (2014) Ligand characteristics and in situ generation of Pd active species towards CC coupling using series of 2-(1H-imidazol-2-yl)phenols. J Mol Catal A Chem 387:112–122. https://doi.org/10.1016/j.molcata.2014.02.032
35. Liu D, Wen L, Chen X et al (2021) Substituent effects on optical properties of pyrrolizine-fused BOPYIN. Spectrochim Acta - Part A Mol Biomol Spectrosc 254:119681. https://doi.org/10.1016/j.saa.2021.119681
36. Zhenglin Y, Shikang W (1993) A study on the photoinduced charge transfer process of triaryl-2-pyrazoline compounds. J Lumin 54:303–308. https://doi.org/10.1016/0022-2313(93)90089-6
37. Singh P, Negi JS, Singh K et al (2012) Synthesis and structure dependent photophysical properties of novel 2-pyrazolines. Synth Met 162:1977–1980. https://doi.org/10.1016/j.synthmet.2012.09.006
38. Fedotov VV, Ulomsky EN, Belskaya NP et al (2021) Benzimidazoazapurines: Design, synthesis, and photophysical study. J Org Chem 86:8319–8332. https://doi.org/10.1021/acs.joc.1c00760
39. Leslie KG, Jacquemin D, New EJ, Jolliffe KA (2018) Expanding the breadth of 4-Amino-1,8-naphthalimide photophysical properties through substitution of the naphthalimide Core. Chem - A Eur J 24:5569–5573. https://doi.org/10.1002/chem.201705546
40. Homg M, Quitevis EL (1993) Excited-state dynamics of polymer-bound J-aggregates. 12408–12415
41. Pochas CM (2018) Extraction of radiative and nonradiative rate constants of super-radiant J-aggregates from emission spectra. J Phys Chem B 122:7185–7190. https://doi.org/10.1021/acs.jpcb.8b04326
42. Shimasaki T, Kobayashi K, Kitanou T et al (2021) Synthesis and photophysical properties of 7-(diethylamino)-3-(4-(arylethynyl) phenyl)-2H-chromen-2-ones as strong fluorescent materials. Tetrahedron 96:132369. https://doi.org/10.1016/j.tet.2021.132369
43. Kahriman N, Ünver Y, Akçay HT et al (2020) Photophysical and photochemical study on novel axially chalcone substituted silicon (IV) phthalocyanines. J Mol Struct 1200:2–11. https://doi.org/10.1016/j.molstruc.2019.127132
44. Saka ET, Göl C, Durmuş M et al (2012) Photophysical, photochemical and aggregation behavior of novel peripherally tetra-substituted phthalocyanine derivatives. J Photochem Photobiol A Chem 241:67–78. https://doi.org/10.1016/j.jphotochem.2012.05.023

45. Tsubone TM, Braga G, Vilsinski BH et al (2014) Aggregation of aluminum phthalocyanine hydroxide in water/ethanol mixtures. J Braz Chem Soc 25:890–897. https://doi.org/10.5935/0103-5053.20140058